Auton Robot
DOI 10.1007/s10514-007-9077-0

Frequency response method for terrain classification in autonomous ground vehicles

Edmond M. DuPont · Carl A. Moore · Emmanuel G. Collins, Jr. · Eric Coyle

Received: 10 September 2006 / Accepted: 5 December 2007

Abstract Many autonomous ground vehicle (AGV) missions, such as those related to agricultural applications, search and rescue, or reconnaissance and surveillance, require the vehicle to operate in difficult outdoor terrains such as sand, mud, or snow. To ensure the safety and performance of AGVs on these terrains, a terrain-dependent driving and control system can be implemented. A key first step in implementing this system is autonomous terrain classification. It has recently been shown that the magnitude of the spatial frequency response of the terrain is an effective terrain signature. Furthermore, since the spatial frequency response is mapped by an AGV's vibration transfer function to the frequency response of the vibration measurements, the magnitude of the latter frequency responses also serve as a terrain signature. Hence, this paper focuses on terrain classification using vibration measurements. Classification is performed using a probabilistic neural network, which can be implemented online at relatively high computational speeds. The algorithm is applied experimentally to both an ATRV-Jr and an eXperimental Unmanned Vehicle (XUV) at multiple speeds. The experimental results show the efficacy of the proposed approach.

Keywords Terrain classification · Autonomous ground vehicles · Probabilistic neural network

E.M. DuPont (✉)
Department of Electrical and Computer Engineering, FAMU-FSU College of Engineering, 2525 Pottsdamer Street, Tallahassee, FL 32310, USA
e-mail: edupont@eng.fsu.edu

C.A. Moore · E.G. Collins, Jr. · E. Coyle
Department of Mechanical Engineering, FAMU-FSU College of Engineering, 2525 Pottsdamer Street, Tallahassee, FL 32310, USA

C.A. Moore
e-mail: camoore@eng.fsu.edu

E.G. Collins, Jr.
e-mail: ecollins@eng.fsu.edu

E. Coyle
e-mail: ejc06c@fsu.edu

1 Introduction

Autonomous ground vehicles (AGVs) are expected to operate in collaboration with manned vehicles in operations including agricultural applications, search and rescue missions, reconnaissance and surveillance, supply and logistics, etc. These situations may require the vehicle to traverse a variety of off-road terrains that can have an affect on the vehicle performance. Therefore, terrain-based adjustments to the vehicle driving rules (Allen 2002; Delong 2000) and control system (Vanderwerp 2005) can improve its performance and prevent the robot from becoming disabled. As an illustration of off-road driving rules in loose sand, the turn radius of a vehicle should be limited and the vehicle should not be allowed to lose momentum (Allen 2002). A terrain-dependent control system is currently available for the Land Rover LR3 (Vanderwerp 2005). This *Terrain Response System* allows the driver to manually adjust the vehicle's control system, including traction control, anti-lock braking, throttle response, transmission shift schedule and differential locking, to achieve improved vehicle handling and performance on four sets of terrains: asphalt, grass/gravel/snow, mud and ruts, and sand.

The first step in automating terrain-dependent driving rules and control systems is automated terrain classification. Initially, research for terrain classification focused almost exclusively on applying vision-based algorithms to infer the traversability and class of the terrain (Howard and

Seraji 2001; Vandapel et al. 2004). The purpose was to identify the terrain prior to traversal to avoid hazardous terrains and obstacles. For example, Howard and Seraji introduced the Fuzzy Traversability Index Algorithm, which used visual intensity levels to determine the terrain characteristics such as the roughness, slope, and discontinuity (Howard and Seraji 2001). These characteristics are used to determine whether the terrain is traversable in relation to the presence of ditches, rocks, or extreme slopes. Detection of the terrain characteristics becomes difficult and unreliable when the effects of shadows affect the ability to distinguish between the terrain surface and obstacles located on the terrain. Another classification method by Vandapel avoids the effects of variability in light intensity by the use of statistical properties of 3D ladar sensor data to detect the surrounding terrains (Vandapel et al. 2004). This method applied off-line statistical analysis techniques to ladar sensor data to segment a scene into three classes: vegetation, terrain rocks, and thin wires or tree branches.

More recent vision-based algorithms have focused on classification of the specific terrain (Angelova et al. 2007; Bradley et al. 2004; Lu et al. 2008) such as gravel, sand, grass, etc., which is the subject of this paper. However, vision-based methods by themselves can be unreliable. For example, if a surface is covered by a thin layer of leaves or the vision sensor is obstructed, vision-based algorithms may have difficulty. These methods may also have difficulty in distinguishing between terrains that look very similar, but are very different from a control perspective, e.g., loose dry sand vs. wet sand or dry pavement vs. wet pavement. Human drivers handle these ambiguities, hence increasing their accuracy in terrain classification, by relying on feel in addition to sight. The goal of this research is to enable AGVs to have a similar sense of feel by developing terrain classification based on proprioceptive sensors such as accelerometers and gyroscopic rate sensors. Hence, this research complements existing terrain classification approaches based on vision.

Past research in terrain classification through feel characterized the terrain by estimating its cohesion and internal friction from measured parameters of the vertical load, torque, wheel sinkage, wheel angular speed, and wheel linear speed (Iagnemma et al. 2002, 2004). These measurements were used in simplified forms of classical terramechanics equations to estimate terrain parameters for planetary rovers, which were compared to stored parameters of known terrains. The equations on which the method is based are effective at low speeds and may encounter issues in parameter measurements such as wheel sinkage in non-granular type terrains. There have been efforts to improve the estimation for use on higher speed vehicles by incorporating vision and auditory based classification with the terrain parameter estimation technique (Iagnemma and Dubowsky 2002).

This paper presents a method that characterizes the terrain by the measured frequency response of the vehicle vibrations. It assumes that the vehicle vibrations are correlated to the terrain type and the terrain signature is given by the magnitude frequency responses of the vibration sensors. An offline set of frequency response data previously recorded from each terrain type is statistically compared to the online measured frequency response data using a probabilistic neural network (PNN); a match between the two sets is used to estimate the current terrain. In previous research the frequency response approach, which was initially suggested in (Iagnemma and Dubowsky 2002) and first developed in (Sadhukan and Moore 2003; Sadhukhan 2004; DuPont et al. 2005), treated the vehicle as a particle with only one degree of freedom. This classification was carried out statistically using a PNN. Similar results for classifying sand, dirt, and gravel were obtained by applying linear discriminant analysis to the power spectral density of vibration data (Brooks et al. 2002). However, treating the vehicle as a particle results in poor performance at certain speeds and on certain terrains, especially when the vibration amplitudes are low.

Recent research also classified and characterized the terrain using individual types of sensor modalities (Ojeda et al. 2006). The experiments were conducted using Activmedia's skid steered Pioneer 2 AT robot platform, with sensor modalities that included an inertial navigation system, motor current sensors, encoders and a microphone sensor. These sensors measured the vehicle responses as the robot traversed grass, sand, gravel, and pavement. Experiments were conducted using data collected as the robot traversed along a 4 m $\times$ 4 m square path at a single speed of 30 cm/s. A multilayered feed-forward network classification system was applied to the extracted discrete Fourier transform frequency components from each individual sensor modality to return a terrain type. Implementation of this approach requires a separate neural network for each sensor modality. In this aspect, each network would return a separate terrain type, which requires an additional classification fusion algorithm to provide an overall resulting terrain type. The fusion of data from all sensor modalities into a single multilayered feed-forward neural network results in a considerable increase in memory and computation requirements, which will result in slow classification.

It has recently been shown that the terrain signature is contained in the magnitude of the spatial frequency response of the terrain (Lu et al. 2008). The terrain can be viewed as providing time-varying inputs to the wheels of the vehicle. The frequency responses of these inputs are directly related to the spatial frequency response of the terrain and are mapped via the vehicle's vibration transfer function to the frequency responses of the vibration sensors. The result is the magnitude of these latter frequency responses serve

as speed-dependent terrain signatures. This paper assumes that the vibration transfer function is unknown and focuses on terrain classification using vibration sensors. A classification approach based on using the vibration transfer function is given in (Collins and Coyle 2008).

In contrast to previous research, the algorithm developed in this paper models the vehicle as a vibration system with three degrees of freedom. The Fast Fourier Transform (FFT) is applied to extract the magnitude frequency components, which together serve as the terrain signature feature vector. The classification is carried out statistically on these signature features using a PNN, which can be implemented online with relatively fast computations. The developed classification algorithm is implemented experimentally on both an ATRV-Jr and an eXperimental Unmanned Vehicle (XUV) at multiple speeds to show the efficacy of the proposed approach.

This paper is organized as follows. Section 2 presents the proposed terrain classification approach. Section 3 presents experimental results. Section 4 discusses mechanisms for improving the algorithm performance. Finally, Sect. 5 presents conclusions.

2 The proposed vibration-based classification approach

This section first considers the basic concepts and assumptions for the proposed vibration-based classification scheme. It then details the proposed method, which uses a PNN as the classifier. Subsequently, the basic operation of the PNN is described.

2.1 Basic concepts and assumptions for vibration-based classification

An unmanned ground vehicle can be modeled as a vibrating system (von Scheidt et al. 1999) with base excitation as illustrated in Fig. 1, which shows the body-centered x-y-z axes. Due to the irregular surface of the terrain, time-varying vertical displacements $X_1(t)$, $X_2(t)$, $X_3(t)$, and $X_4(t)$ occur at each of the wheels. If these displacements can be measured, then they could be used for terrain classification. However, these displacements are difficult or impossible to measure in real time. Instead the vibration of the vehicle as a single body can be measured using proprioceptive sensors, such as those available as part of an internal navigational unit (Sukarrieh 2000). The vibration due to the vertical wheel displacements is completely characterized by the vertical, roll, and pitch motions and here are considered to be the vertical acceleration $\ddot{z}(t)$, the pitch rate $\omega_y(t)$, and the roll rate $\omega_x(t)$.

A numerical model for the system of Fig. 1 was obtained using four simplifying assumptions. First, the center of gravity is located in the geometric center of the robot. Second,

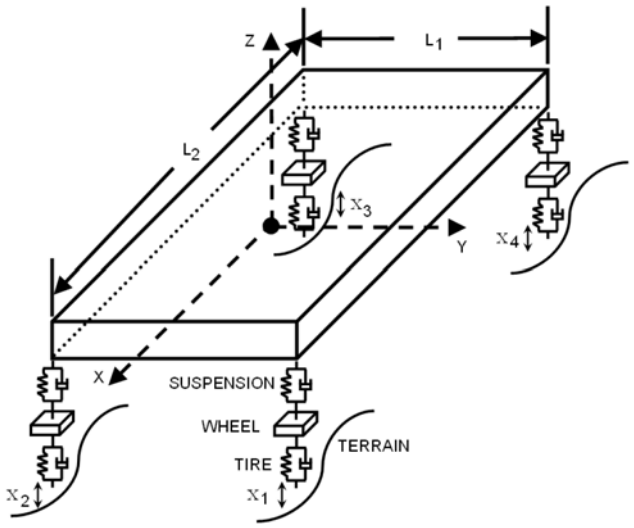

Fig. 1 Vehicle Model: A vibrating system with base excitation

the body mass includes the mass of the tires. Third, the motion is limited to small angles, which enabled the development of a linear model. Lastly, the tires maintain contact with the ground and the tire geometry is ignored. Based on these assumptions the system reduces to the model,

$$\begin{bmatrix} \ddot{z}(s) \\ \omega_y(s) \\ \omega_x(s) \end{bmatrix} = \underbrace{\begin{bmatrix} g_{11} & g_{12} & g_{13} & g_{14} \\ g_{21} & g_{22} & g_{23} & g_{24} \\ g_{31} & g_{32} & g_{33} & g_{34} \end{bmatrix}}_{G(s)} \begin{bmatrix} X_1(s) \\ X_2(s) \\ X_3(s) \\ X_4(s) \end{bmatrix}, \tag{1}$$

where

$$g_{11} = g_{12} = g_{13} = g_{14} = \frac{cs^3 + ks^2}{ms^2 + 4cs + 4k},$$

$$g_{21} = g_{22} = \frac{\frac{L_2}{2}cs^2 + \frac{L_2}{2}ks}{I_y s^2 + L_2^2 cs + L_2^2 ks},$$

$$g_{23} = g_{24} = \frac{-\frac{L_2}{2}cs^2 - \frac{L_2}{2}ks}{I_y s^2 + L_2^2 cs + L_2^2 ks}, \tag{2}$$

$$g_{31} = g_{34} = \frac{\frac{L_1}{2}cs^2 + \frac{L_1}{2}ks}{I_x s^2 + L_1^2 cs + L_1^2 ks},$$

$$g_{32} = g_{33} = \frac{-\frac{L_1}{2}cs^2 - \frac{L_1}{2}ks}{I_x s^2 + L_1^2 cs + L_1^2 ks},$$

where m is the mass of the robot, I_x and I_y are respectively the mass moment of inertias about the x-axis and y-axis, and c and k are respectively the damping and spring constants of the tires.

The terrain signature is given by $|X(j\omega)|$ as shown in (Lu et al. 2008). However, it is impossible or extremely difficult to directly measure $|X(j\omega)|$ using proprioceptive sen-

sors. What may be obtained is the frequency responses corresponding to the vibration measurements $\ddot{z}(t)$, $\omega_y(t)$ and $\omega_x(t)$. Denote the magnitudes of the corresponding FFTs by the column vectors $\mathbf{f}_{\ddot{z}}$, $\mathbf{f}_{\omega_x}$ and $\mathbf{f}_{\omega_y}$. Then, it is assumed in this paper that the terrain signature is the feature vector

$$\mathbf{t} = \begin{bmatrix} \mathbf{f}_{\ddot{z}} \\ \mathbf{f}_{\omega_x} \\ \mathbf{f}_{\omega_y} \end{bmatrix}. \tag{3}$$

Of course, $\mathbf{t}$ is dependent upon the transfer function $G(s)$, which is assumed unknown in this paper. Changes to the body of the vehicle, such as load variations or tire pressure, will lead to changes in $G(j\omega)$, which will in turn lead to a change in the signature vector $\mathbf{t}$. As an illustration, consider the case in which results from (Wong 2001) are used to choose the mass, stiffness and damping parameters in (2) to correspond to the ATRV-Jr, which has a specified maximum load capacity of 25 kg. Figure 3 shows the variations in the magnitude of four of the elements of $G(j\omega)$ as the carried load, assumed to be concentrated above the center of gravity, varies from 0 kg to 25 kg. Obviously, these variations have the potential to effect classification based on $\mathbf{t}$.

In classifying the traversed terrain there are two possible ways to address the affects of a changing load. The most straightforward approach is to collect additional samples to train the algorithm under multiple expected load conditions. However for a robot with a large range of carrying capacity this could result in an unreasonably large training set. A second approach is to amplify or attenuate the elements of $\mathbf{t}$ based on the known load and tire pressures. If a reliable analytical model of the vehicle is known, this approach is preferable since the training set would require a reduced number of samples without significantly affecting the online classification time. Research on these approaches is currently being conducted, but is not presented in this paper.

Fig. 2 iRobot ATRV-Jr robot platform

2.2 The proposed algorithm

The four fundamental elements of statistical based classification are the choice of the sensor inputs, preprocessing of the sensor data, feature extraction, and classification (Jain et al. 2000). As shown in Fig. 4, in this research the sensor inputs were the vehicle speed and the vibration measurements ($\ddot{z}$, ω_y, and ω_x) over a fixed time interval. These measurements were obtained from an inertial navigation unit. The preprocessing of the data involved taking the FFT of the vibration measurements. The magnitude of the combined FFT vectors in $\mathbf{t}$ was extracted as the features to be used for classification. Actual classification was then accomplished using a PNN that was trained at the measured speed.

Figures 5, 6, and 7 display examples of the magnitudes of the FFTs obtained for the ATRV-Jr traveling at a constant speed of 0.5 m/s over the following surfaces: packed gravel, loose gravel, sparse grass, tall grass, asphalt, and beach sand.

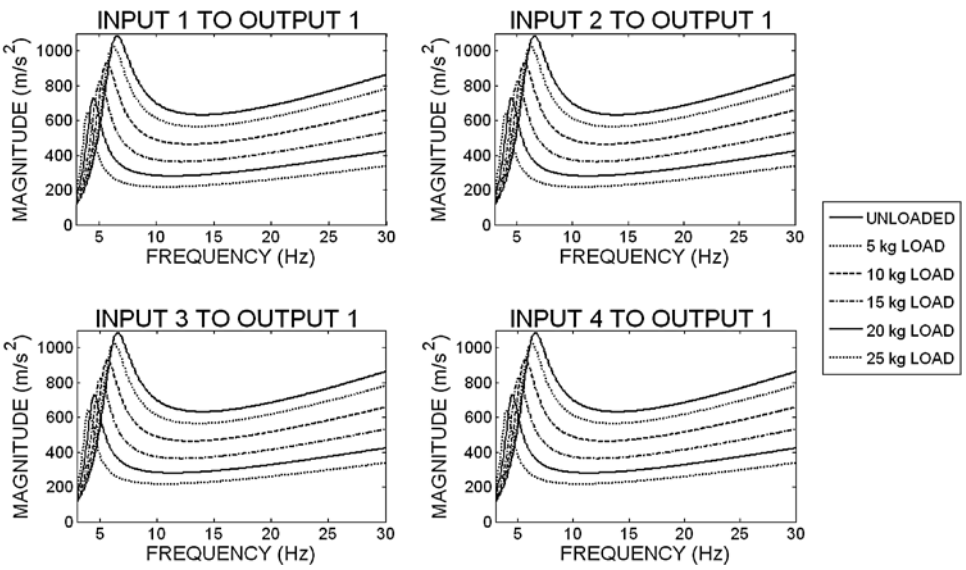

Fig. 3 An example of the changes in magnitude of $G(j\omega)$ along $\ddot{z}$ for changes in vehicle's load mass

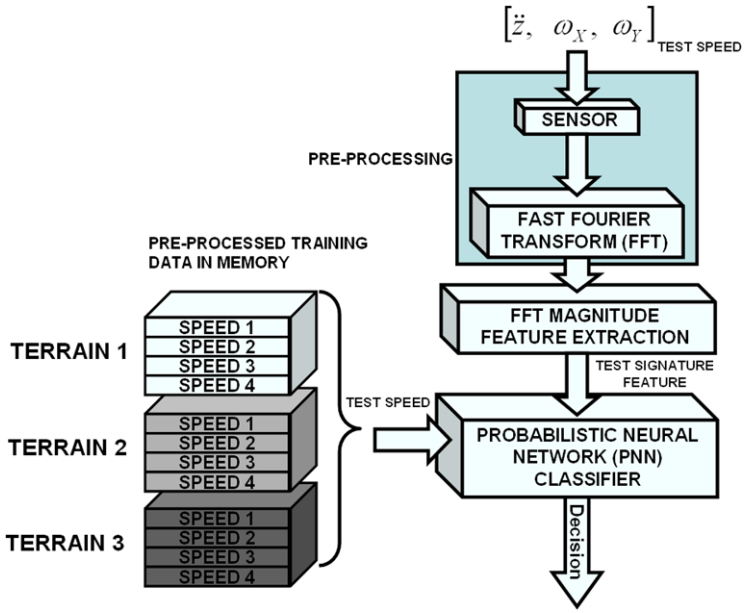

Fig. 4 The speed dependent classification system

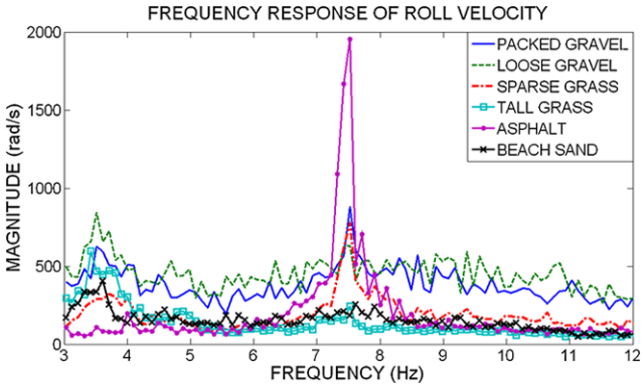

Fig. 5 The magnitude frequency response of the x-axis rotation rate as the vehicle traveled over the six terrains

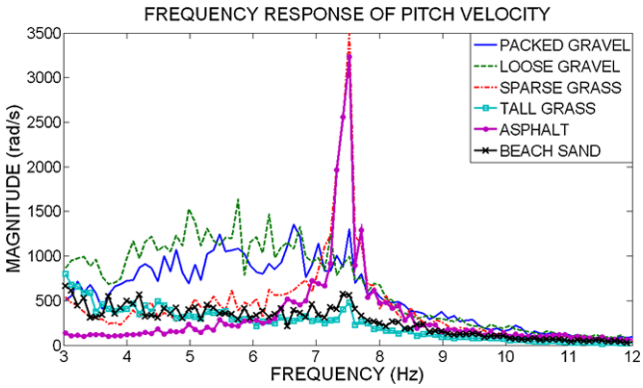

Fig. 6 The magnitude frequency response of the y-axis rotation rate as the vehicle traveled over the six terrains

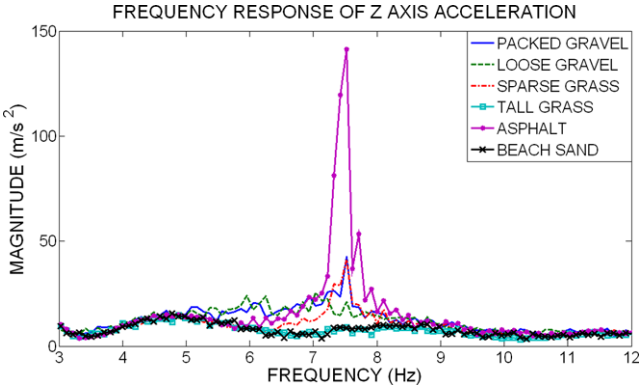

Fig. 7 The magnitude frequency response of the z-axis acceleration as the vehicle traveled over the six terrains

Each terrain produced a substantially unique FFT magnitude in the frequency range [3, 30] Hz. However, for visual clarification the figures only show the responses in the interval [3, 12] Hz. The FFT magnitudes of Figs. 5, 6, and 7 respectively define the vectors $\mathbf{f}_{\ddot{z}}$, $\mathbf{f}_{\omega_x}$ and $\mathbf{f}_{\omega_y}$, which as discussed above are the single terrain feature vector $\mathbf{t}$, defined by (3). To train the PNN the feature vector $\mathbf{t}$ is computed using multiple samples at various speeds along the different terrains. This data is stored in the PNN memory as the preprocessed training data.

The online classification procedure corresponds to determining a best fit for a new unknown input test vector $\mathbf{t}$ within a region of a high dimensional vector space. To enable some visualization of the classification process, Fig. 8 shows the elements of the feature vectors $\mathbf{f}_{\ddot{z}}$, $\mathbf{f}_{\omega_x}$ and $\mathbf{f}_{\omega_y}$ corresponding to the frequency of 7.5195 Hz; this frequency was chosen because the magnitude frequency responses of Figs. 5, 6, and 7 tend to have high amplitude at this frequency. In particular, Fig. 8 shows a scatterplot representation for the six terrains with five samples for each terrain. The data clustering for each of the terrains is evident in Fig. 8. There is clearly some separation between terrains, which is especially evident for asphalt, packed gravel, loose gravel, and

sparse grass. It is also evident that beach sand and tall grass appear to be closely adjoined. Note that the actual dimension of the feature vector $\mathbf{t}$ is 831 ($= 277 \times 3$). In general, more separation between these two terrains is seen in this higher dimensional space. However, as seen below in Table 1, even in the higher dimensional space, tall grass is occasionally mistaken for sand.

2.3 Probabilistic neural network classification

This section describes how the PNN was used to classify an unknown test feature vector $\mathbf{t}$ as a particular terrain. Several tools such as the backpropagation multilayer perceptron, support vector machines, and other similar methods for pattern classification could have been used (Michie et al. 1994; Tsoukalas and Uhrig 1997). The PNN was chosen because of its simplicity, robustness to noise, fast online training, and fast online classification (Specht 1990a).

The PNN (Specht 1990a, 1990b) is a pattern classifier that applies classical Bayes optimal decision theory. The

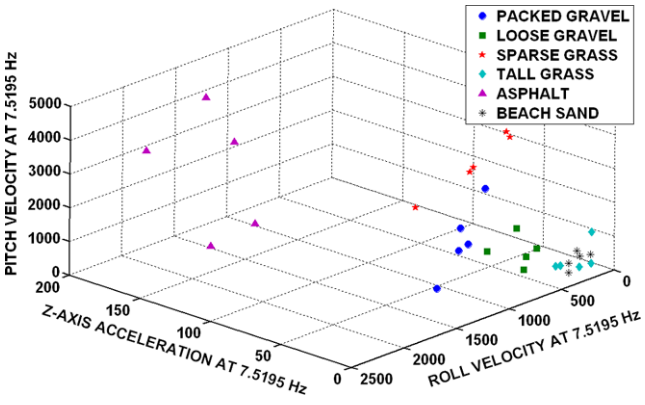

Fig. 8 Terrain vector space point cloud representation using the dominant frequency 7.5195 Hz of along all the terrains

Bayes decision rule states that an unknown vector $\mathbf{t}$ is assigned to class c_i of a two category case as

$$h_i l_i P(c_i|\mathbf{t}) > h_j l_j P(c_j|\mathbf{t}), \quad i \neq j, \tag{4}$$

where h_k is the prior probability of occurrence, l_k is the loss associated with misclassifying an object to class k, and $P(c_k|\mathbf{t})$ is the probability density function (pdf) of $\mathbf{t}$ belonging to class k. The PNN simplifies this decision rule by assuming that the prior probability h_k and the loss function l_k are equal for all categories; therefore, the decision is based entirely on the pdf, which reduces (4) to

$$P(c_i|\mathbf{t}) > P(c_j|\mathbf{t}), \quad \forall i \neq j. \tag{5}$$

A known limitation of (5) is that the pdf of $\mathbf{t}$ for all classes is not known, meaning (5) cannot be directly implemented. The PNN avoids this problem by applying the Parzen-windows approach, which uses random samples of the classes in conjunction with the unknown test sample to approximate the probability distribution functions (Parzen 1962; Murthy 1965, 1966; Cacoullos 1966). The feed-forward neural network structure of the PNN classifier, shown in Fig. 9, consist of an input layer, pattern layer, summation layer, and output layer. The input layer distributes the unknown test input vector $\mathbf{t}$ to the pattern layer after applying a weight that is the training vector j of class i as $\mathbf{t}_j^i$ yielding

$$z_j^i = \mathbf{t}^T \mathbf{t}_j^i, \tag{6}$$

where z_j^i represents the input to each pattern neuron j of class i.

The exponential function $\exp[-(z_j^i - 1)/\sigma^2]$ is applied to the input z_j^i as the nonlinear activation function instead of the commonly known sigmoid function used by typical multi-layered feed-forward networks. This activation

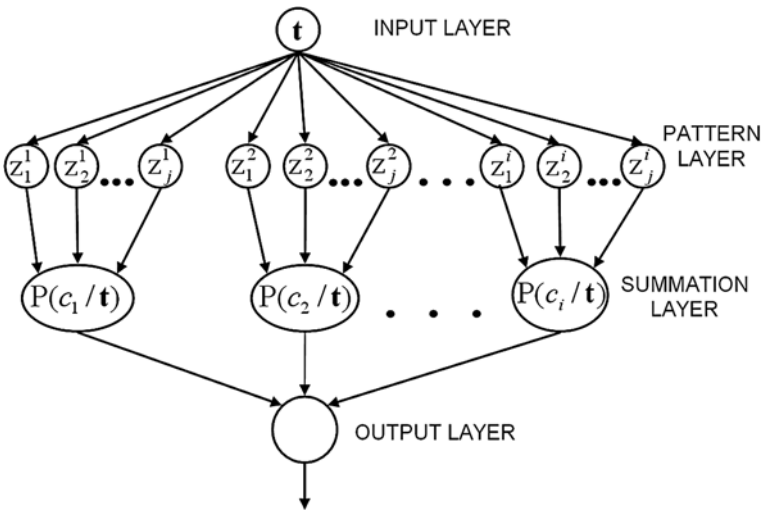

Fig. 9 The structure of probabilistic neural network

function represents a Gaussian distribution centered at each training vector for each class. The summation layer applies a unit scaled weight to each neuron received from the pattern layer and sums the inputs corresponding to the class of the training features. The summation layer applies the Parzen-window estimator to compute the probability of a given input $\mathbf{t}$ belonging to a class c_i, with the nonlinear exponential as the window function. This results in the approximation,

$$P(c_i|\mathbf{t}) = \frac{1}{(2\pi)^{\frac{N}{2}}\sigma^N n_i} \sum_{j=1}^{n_i} \exp\left[\frac{-(z_j^i - 1)}{\sigma^2}\right], \tag{7}$$

where $\sigma > 0$ is known as the smoothing parameter defining the window width, N is the dimension of the input vectors, and n_i is the number of sample patterns in class i. This represents an average of density estimates for each class that is then scaled by the reciprocal of the window function volume. The output layer uses the calculation of the pdf from the summation layer, and applies the decision rule of (5) to select the class with highest probability.

An issue associated with applying the PNN classifier is choosing a suitable estimate of the smoothing parameter σ. This parameter defines the decision boundaries between the trained categories. As σ increases, the decision boundaries becomes highly linear and can result in an overlap of closely related classes. On the other hand, a value of σ too small results in very non-linear boundaries behaving as the nearest neighbor classifier, which does not result in optimal class separation. It is not difficult to find a suitable value of σ and the misclassification rate is not significantly impacted with small changes (Specht 1988). There exist different approaches to choosing a suitable smoothing parameter σ such as the hold-one-out cross-validation approach, in which σ is selected to maximize the performance across all classes within a predefined range for given test inputs. The inputs consist of cyclically removing one training data sample to use as a testing input or having an entirely separate cross-validation dataset. In these initial experiments, the smoothing parameter was chosen empirically, but future experiments will implement the cross-validation technique.

3 Field experimentation

The classification algorithm described in Sect. 2 was programmed in Matlab and implemented off-line. It was first applied to data collected from the ATRV-Jr, a differentially steered vehicle that has no suspension system, weighs about 50 kg, and has a maximum traversal speed of 1.4 m/s. Next, the classification algorithm was applied to data collected on the much larger XUV, a four wheel steered vehicle with an independent suspension system on each wheel that weighs approximately 1150 kg and has a maximum speed of about 40 mph, although the experiments were limited to speeds not exceeding 20 mph.

3.1 Experiments and results for the ATRV-Jr

The ATRV-Jr, shown in Fig. 2, was equipped with an onboard computer powered by a Pentium 3 800 MHz processor running the Red Hat Linux 6.2 operating system. Although various sensors were mounted on the ATRV-Jr robot platform, this classification research focused on data measured from the inertial measurement unit (IMU). As shown in Fig. 10, the IMU is mounted within the body of the robot centered underneath the onboard computer; it measures the vehicle's translational accelerations and the rotational velocities of the vehicle about the body fixed coordinate axes.

As shown in Fig. 11, the robot was commanded to traverse six different terrains: asphalt, packed gravel, loose gravel, tall grass, sparse grass, and beach sand. For each terrain the IMU recorded $\ddot{z}$, ω_y, and ω_x at ground speeds of 0.5 m/s and 1 m/s in 10-second intervals at a sample rate of 200 Hz resulting in 2000 time domain samples. A uniform windowed FFT was applied to each 10-second time signal and the magnitude frequency components were extracted. The transformation produced magnitudes at 277 of the total 2048 frequency points along each axes within the frequency range [3,30] Hz. This frequency range contained the domi-

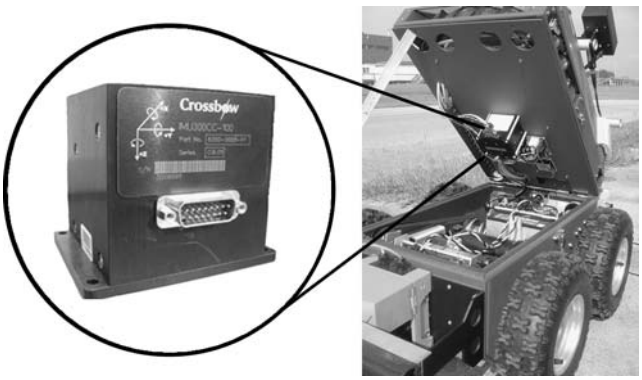

Fig. 10 Crossbow IMU sensor for measuring gyro rates and accelerations along the vehicle's principal axes

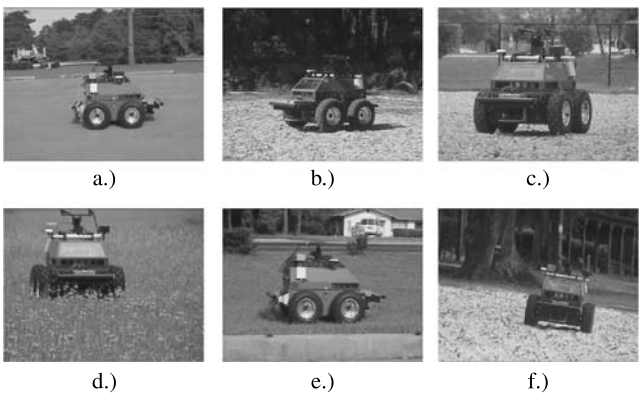

Fig. 11 Robot traversing **a** asphalt, **b** packed gravel, **c** loose gravel, **d** tall grass, **e** sparse grass, and **f** sand

Table 1 Terrain classification results at 0.5 m/s

Tested Terrain	Detected Terrain					
	Packed Gravel	Loose Gravel	Sparse Grass	Tall Grass	Asphalt	Sand
Packed Gravel	100%					
Loose Gravel	26.7%	73.3%				
Sparse Grass			100%			
Tall Grass				93.3%		6.7%
Asphalt					100%	
Sand						100%

Table 2 Terrain classification results at 1 m/s

Tested Terrain	Detected Terrain					
	Packed Gravel	Loose Gravel	Sparse Grass	Tall Grass	Asphalt	Sand
Packed Gravel	86.7%	13.3%				
Loose Gravel	26.7%	73.3%				
Sparse Grass			93.3%	6.7%		
Tall Grass				100%		
Asphalt					100%	
Sand						100%

nant signature magnitude components across all the terrains. This resulted in a 831-dimensional feature vector for each terrain. These vectors were stored in memory as the training data for the PNN classifier.

Testing the algorithm consisted of inputting additional data of the robot traversing the test terrains for 150 seconds and measuring $\ddot{z}$, ω_y, and ω_x at the same sample rate as the training data. This data was also divided into 10 second segments and the frequency components were extracted similar to that of the training data. Each of the test samples were applied as inputs to the classification system to calculate the probability that the test feature vector belongs to a particular trained class. The algorithm produced 15 resulting terrain classifications given that the 150 second feature vector is evaluated every 10 seconds.

Tables 1 and 2 present the classification results at the speeds of 0.5 m/s and 1 m/s, respectively, for all of the terrains. The results show a high ability to distinguish between the trained terrains. For example, at 0.5 m/s speed, the algorithm classified five of the six terrains with greater than 90% accuracy. At 1.0 m/s these same five terrains were classified with greater than 85% accuracy. Tall grass misclassified one of the input samples as beach sand at 0.5 m/s, but provided a perfect classification at 1 m/s. Although at 0.5 m/s, one sample of the sparse grass was misclassified as tall grass, the algorithm did classify this sample as a grass terrain. Similar classifications results were evident in distinguishing between the gravel terrains. In general the loose gravel provided more tire sinkage than the packed gravel. However, this effect was not consistent throughout the loose gravel area. As a result, the classification algorithm sometimes confused the two types of gravel surfaces. The asphalt and sand terrains resulted in perfect classification performance.

It should be noted that since the goal of this research is to alter the robot's driving and control based on terrain, it is not necessary to distinguish between all terrain types. Instead, it is sufficient to distinguish between terrain classes that require unique driving rules and control. For example, since the loose and packed gravel are nearly identical, they may not require dissimilar control. Nevertheless, they were treated separately in these experiments to test the algorithm's ability to distinguish between terrains that are nearly identical in appearance and roughness.

3.2 Experiments and results for the XUV

The required XUV data was provided by its Inertial Reference Unit (IRU), which measured the rotation rates and accelerations about the three axes, at an update rate of 50 Hz. The XUV traversed asphalt, gravel, grass, mud and dirt at speeds of 5 mph, 8 mph, 11 mph, 14 mph, 17 mph, and 20 mph. With the goal of classifying terrains that require dissimilar control strategies, the grass and gravel terrains were combined into one terrain type, consistent with the Land Rover Terrain Response System (Vanderwerp 2005). Hence, the number of terrain types considered was actually four: asphalt, gravel/grass, mud and dirt. The data collection for the XUV differed substantially from the data collection for the ATRV-Jr in that some of the data was collected while the vehicle was accelerating. This was necessitated by limits on the traversable distance at the experimental test grounds.

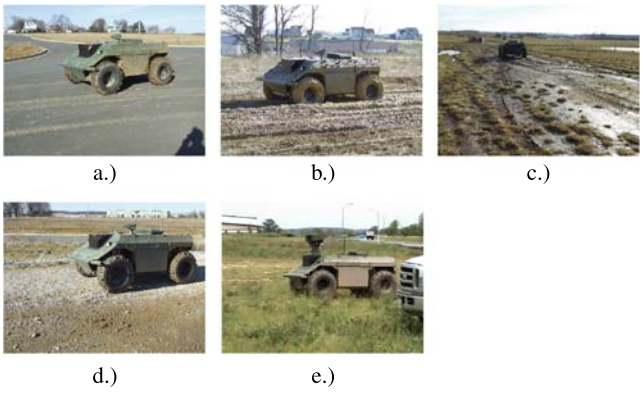

Fig. 12 XUV Robot traversing **a** asphalt, **b** mud, and **c** dirt, **d** gravel, **e** and grass, respectively

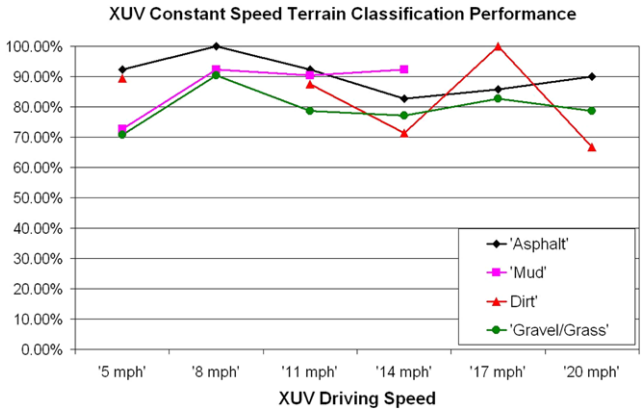

Fig. 13 The results of applying the speed dependent classification system on data collected from the XUV robot platform

Figure 13 shows the results of applying the classification system on the data collected and divided into 2 second samples. The number of samples varied depending on the speed and terrain traversed.

The terrain classification accuracy was in the range [70%,100%] for each of the terrain/speed combinations except one (dirt at 20 mph which was classified at 65% accuracy). It is important to note that unlike the ATRV-Jr which has no suspension, the XUV suspension effectively damps outs some of the vibration signatures that would otherwise be significant for classification. The classification of mud improved as the speed increased due to the influence of the ruts on the angular velocities during data collection.

4 Discussion on algorithm improvements

Common classification systems involve an offline training procedure and online classification. The classification presented here applies a training procedure that can be implemented online although it was implemented offline in Matlab in this research. The effective preprocessing of this training data is conducted offline and stored within the system memory. In Matlab, this classification system's "online procedure" resulted in an average of 150 ms processing time to return the resulting terrain of a 10 second sample. This computation time will reduce considerably when developed in a real-time environment for actual implementation. This computation time can also be reduced by using a reduced set of training samples and reducing the dimensions of the feature vector. This dimension reduction has been performed by using the Principal Component Analysis feature extraction technique (DuPont et al. 2006). In addition, research presented in (DuPont et al. 2006) reduced the sample time segments from 10 seconds to 2 seconds.

Additional algorithm improvements can be obtained by estimating the smoothing parameter σ using approaches such as jackknifing and cross-validation (Masters 1993). This estimation procedure would be included within the offline processing of the training data and would not affect the online computational time.

Improving the classification performance may also be achieved by the inclusion of additional sensor features that provide additional characteristics of the terrain. These sensors may include measurement of wheel slip, which will help to distinguish high slip terrains such as mud, ice and snow from lower slip terrains.

The addition of an unclassifiable threshold technique is also needed to distinguish terrains that the PNN classifier has not been trained to recognize (Washburne et al. 1993). These terrains should be reported as unclassifiable. However, in the current implementation, the algorithm returns a classification based on training classes with the largest probability . This can result in false positive detection instead of the preferred reporting of an unknown result.

5 Conclusions

This article focused on the development of an AGV terrain classification algorithm that applied the probabilistic neural network classifier on the extracted frequency responses of terrain induced vehicle vibrations. This inherently fast algorithm shows promise in the explicit identification of various terrains. Experiments on an ATRV-Jr, a vehicle without a suspension system, revealed high performance results in classifying six traversed terrains at different speeds. In addition, the classification algorithm was applied to data extracted from the XUV, a much larger vehicle that has a suspension system, which tends to reduce the magnitude and hence the observability of the terrain vibration signatures. Although, the classification system produced reasonable performance, the addition of other sensor measurement features, such as wheel slip, should improve the classification accuracy. Future research should also include the implementation of a probability confidence threshold to indicate

the reliability of the classification decision, which should reduce false positive identifications.

References

Allen, J. (2002). *Four-wheeler's bible*. St. Paul: MotorBooks.

Angelova, A., Matthies, L., Helmick, D., & Perona, P. (2007). Fast terrain classification using variable-length representation for autonomous navigation. In *Proceedings of the IEEE conference on computer vision and pattern recognition (CVPR)* (pp. 1–8).

Bradley, D., Thayer, S., Stentz, A., & Rander, P. (2004). *Vegetation detection for mobile robot navigation* (Technical Report CMU-RI-TR-04-12). Robotics Institute, Carnegie Mellon University, Pittsburgh, PA, February 2004.

Brooks, C., Iagnemma, K., & Dubowsky, S. (2002). Vibration-based terrain analysis for mobile robots. In *Proceedings of the IEEE international conference on robotics and automation (ICRA)* (pp. 3142–3147), Barcelona, Spain, May 2002.

Cacoullous, R. (1966). Estimation of a probability density. *Annals of the Institute of Statistical Mathematics (Tokyo)*, *18*(2), 179–189.

Collins, E. G., Jr., & Coyle, E. (2008, to appear). Vibration-based terrain classification using surface profile input frequency responses. In *International conference on robotics and automation*. Available at http://www.eng.fsu.edu/ciscor/publications.htm.

Delong, B. (2000). *4-wheel freedom: the art of off-road driving*. Boulder: Paladin.

DuPont, E. M., Roberts, R. G., Moore, C. A., Selekwa, M. F., & Collins, E. G., Jr. (2005). Online terrain classification for mobile robots. In *Proceedings of the ASME international mechanical engineering congress and exposition conference*, Orlando, FL, November 2005.

DuPont, E. M., Roberts, R. G., & Moore, C. A. (2006). Speed independent terrain classification. In *Proceedings of the 38th southeastern symposium on system theory*, Cookeville, TN, March 2006.

Howard, A., & Seraji, H. (2001). Vision-based terrain characterization and traversability assessment. *Journal of Robotic Systems*, *18*(10), 577–587.

Iagnemma, K., & Dubowsky, S. (2002). Terrain estimation for high speed, rough-terrain autonomous vehicle navigation. In *Proceedings of the SPIE conference on unmanned ground vehicle technology* (pp. 256–266), Orlando, FL, May 2002.

Iagnemma, K., Shibly, H., & Dubowsky, S. (2002). Terrain parameter estimation for planetary rovers. In *Proceedings of the IEEE international conference on robotics and automation (ICRA)* (pp. 3142–3147), Washington, DC, May 2002.

Iagnemma, K., Kang, S., Shibly, H., & Dubowsky, S. (2004). Online terrain parameter estimation for wheeled mobile robots with application to planetary rovers. *IEEE Transactions on Robotics*, *20*(5), 921–927.

Jain, A., Duin, R. P. W., & Mao, J. (2000). Statistical pattern recognition: a review. *IEEE Transactions on Pattern Analysis and Machine Intelligence*, *22*(1), 4–36.

Lu, L., Ordonez, C., Collins, E. G., Jr., & DuPont, E. M. (2008, submitted for publication). Terrain classification for autonomous ground vehicles using 2-D laser stripe-based structured light sensors. In *International conference on robotics and automation*. Available at http://www.eng.fsu.edu/ciscor/publications.htm.

Masters, T. (1993). *Practical neural network recipes in C++*. New York: Academic Press.

Michie, D., Spiegelhalter, D. J., & Taylor, C. C. (1994). *Machine learning, neural and statistical classification*. Chichester: Ellis Horwood. ISBN 0-13-106360-X. URL citeseer.nj.nec.com/michie94machine.html.

Murthy, V. K. (1965). Estimation of a probability density. *Annals of Mathematical Statistics*, *36*, 1027–1031.

Murthy, V. K. (1966). Nonparametric estimation of multivariate densities with applications. In P. R. Krishnaiah (Ed.), *Multivariate analysis* (pp. 43–56). New York: Academic Press.

Ojeda, L., Borenstein, J., Witus, G., & Karlsen, R. (2006). Terrain characterization and classification with a mobile robot. *Journal of Field Robotics*, *23*(2), 103–122.

Parzen, E. (1962). On estimation of a probability density function and mode. *Annals of Mathematical Statistics*, *33*, 1065–1076.

Sadhukhan, D. (2004). *Autonomous ground vehicle terrain classification using internal sensors*. Master's thesis, Departent of Mechanical Engineering, Florida State University, Tallahasee, FL.

Sadhukan, D., & Moore, C. (2003). Online terrain estimation using internal sensors. In *Proceedings of the Florida conference on recent advances in robotics*, Boca Raton, FL, May 2003.

Specht, D. F. (1988). Probabilistic neural networks for classification, mapping, or associative memory. In *Proceedings IEEE international conference on neural networks* (pp. 525–532), San Diego, CA.

Specht, D. F. (1990a). Probabilistic neural networks. *Neural Networks*, *3*(1), 109–118.

Specht, D. F. (1990b). Probabilistic neural networks and the polynomial adaline as complementary techniques for classification. *IEEE Transactions on Neural Networks*, *1*(1), 111–121.

Sukarrieh, S. (2000). *Low cost high integrity aided inertial navigation systems for autonomous land vehicles*. PhD thesis, University of Sydney, Sydney, Australia.

Tsoukalas, L. H., & Uhrig, R. E. (1997). *Fuzzy and neural approaches in engineering*. New York: Willey. ISBN 0-471-16003-2.

Vandapel, N., Huber, D. F., Kapuria, A., & Herbet, M. (2004). Natural terrain classification using 3-d ladar data. In *Proceedings of the IEEE international conference on robotics and automation (ICRA)* (pp. 5117–5122), New Orleans, LA, April 2004.

Vanderwerp, D. (2005). What does terrain response do? http://www.caranddriver.com/features/9026/what-does-terrain-response-do.html.

von Scheidt, J., Wunderlich, R., & Fellenberg, B. (1999). Random road surfaces and vehicle vibration. In L. Arkeryd, J. Bergh, P. Brenner, & R. Pettersson (Eds.), *Progress in industrial mathematics at ECMI 98* (pp. 352–359). Stuttgart: Teubner.

Washburne, T. P., Specht, D. F., & Drake, R. M. (1993). Identification of unknown categories with probabilistic neural networks. In *Proceedings of the IEEE international conference on neural networks* (pp. 434–437).

Wong, J. Y. (2001). *Theory of ground vehicles* (3rd ed.). New York: Wiley.

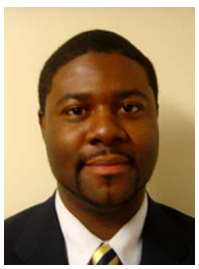

Edmond M. DuPont received his B.S., M.S., and Ph.D. degrees in Electrical Engineering from Florida A&M University in 1999, 2001, and 2007, respectively. He has professional industry experience working with both Motorola and Sony Technology Center. He is currently a research assistant for the Center for Intelligent Systems, Controls and Robotics at the FAMU-FSU College of Engineering. His research interests are in the areas of classification algorithms and sensor data processing for autonomous robot systems.

Carl A. Moore earned his B.S. in Mechanical Engineering from Howard University and his M.S. and Ph.D. from Northwestern University in 2001.
He is currently an Associate Professor in the Department of Mechanical Engineering at Florida A&M University, Tallahassee, FL. He has professional manufacturing experience with Eastman Kodak and research experience with Ford Motor Company. Besides teaching courses in robotics and dynamics, he performs research in the design and control of intelligent mechanical systems. In particular he was instrumental in the development of serial link cobots, a class of robots designed for safe collaboration with humans.
Dr. Moore served on the Robotics Technical Panel for the ASME Dynamic Systems and Control Division.

Emmanuel G. Collins, Jr. is John H. Seely Professor of Mechanical Engineering and Director of the Center for Intelligent Systems, Control and Robotics (CISCOR) at the joint College of Engineering of Florida A&M University and Florida State University. He received his Ph.D. in Aeronautics and Astronautics from Purdue University in 1987 and also holds B.S. degrees from Morehouse College and the Georgia Institute of Technology. He spent 7 years in research and development at the Harris Corporation prior to joining the Department of Mechanical Engineering as an Associate Professor in August 1994. Dr. Collins teaches courses in control, robotics and dynamics. His current research interests are in control and guidance of autonomous vehicles in extreme environments and situations, coordination of teams of heterogeneous agents (including human-robot teams), fault detection and isolation, and applications of modern robust control theory.

Eric Coyle received a B.S. degree in mechanical engineering with a minor in mathematical sciences from Clemson University in May 2006. He is currently pursuing a Ph.D. in Mechanical Engineering at Florida State University with a concentration in Dynamics and Controls. He is working at the Center for Intelligent Systems, Control and Robotics to develop advanced vibration-based terrain classification techniques for wheeled robots. Additionally, he is working with the Human Engineering Research Laboratory to develop hazardous driving rules and automated driver assistance for electric powered wheelchairs. His research interests include rehabilitation engineering, robotics, controls and automation.